

Automated Micro-Assembly of Surface MEMS Mirrors by Centrifugal Force

King W. C. Lai¹, P.S. Chung², Ming Li² and Wen J. Li^{1,*}
¹Centre for Micro and Nano Systems, The Chinese University of Hong Kong
²Photonic Packaging Laboratory, The Chinese University of Hong Kong
Hong Kong SAR

***Abstract**—A very fast, low-cost, and reliable method to assemble micro structures suitable for MOEMS (micro-opto-electro-mechanical systems) applications is reported in this paper. In general, due to the minute scale of MEMS devices, inertia force is often neglected when dealing with MEMS components. However, we have demonstrated that inertia force can be significant even if the mass of micro structure is $<1\mu\text{g}$ (a $250\mu\text{m}\times 100\mu\text{m}$ mass with $3.5\mu\text{m}$ thick polysilicon and $0.5\mu\text{m}$ thick Au layers). At this scale, we have shown that, mass inertia force can overcome some surface forces and thus be used for non-contact self-assembly of MEMS structures. Centrifugal force was applied to MUMPs (Multi-User-MEMS-Processes) chips by attaching the chips to a rotating disc. The micro hinged structures on the chips were shown to self-assemble by rotating themselves 90° out of substrate plane in most cases, and automatically lock themselves to designed latches. The assembly process is also applicable to complex dynamic micro mirror structures. Our experimental setup and systematic approach to acquire force data during the centrifugal assembly process is described in this paper.

Index Terms—micro assembly, batch assembly, automated micro assembly, centrifugal assembly.

I. INTRODUCTION

NEW designs for surface-micromachined devices that require micro-assembly to form 3D structures have focused on the ease of post-fabrication assembly. An example of a simple technique was reported as a single-step assembly by manual probing in [1], where movement of a single plate or structure assembles the entire structure constrained by hinges. Automatic latches have also been used to engage and lock these structures into position. Other techniques to assemble hinged structures include using on-substrate actuators [2], surface tension force [3], and triboelectricity [4]. All these methods have inherent disadvantages such as yield, cost, and difficulty in implementation. In this paper, we propose a fast, low-cost, non-contact, and high-yield batch assembly technique using centrifugal force to lift MEMS structures.

It is generally accepted that surface forces are dominant compare to volume forces for MEMS devices since

surface area reduction is proportional to only $2/3$ power of the reduction in volume according to isometric scaling argument. Consequently, it is often assumed that inertia force is negligible in the presence of other forces such as friction or surface forces. However, our research has proved that mass does matter to a certain scale in MEMS. Our work has demonstrated that the inertia force of many MEMS structures can overcome friction and surface forces. From this, we present a novel non-contact method of batch auto-assembly of surface-micromachined devices that has many advantages over conventional micro-assembling methods.

II. MICRO-ASSEMBLY BY CENTRIFUGAL FORCE

Our setup for centrifugal assembly is shown in Figure 1. Centrifugal force (F) acting on the mass (m) of a micro structure to be assembled is related the angular speed (ω) and radius (r) of a rotation disc by:

$$F = m \cdot r \cdot \omega^2 \quad (1)$$

Centrifugal force is a good choice to perform micro-assembly because the force applied on the micro structures can be evenly distributed so that the micro structures would not be destroyed easily. Since the mass of a typical micro structure is very small, a 3cm radius disc rotating at 6250rpm will generate $\sim 3 \times 10^{-6}\text{N}$ force on a $250\mu\text{m}\times 100\mu\text{m}\times 4\mu\text{m}$ (see Figure 2 for thin film layer

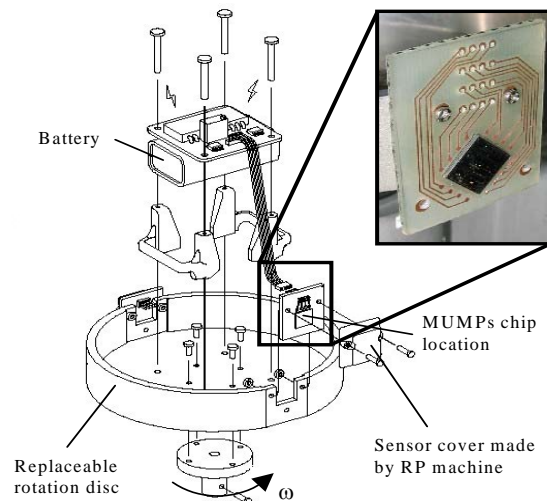


Figure 1. Conceptual drawing of the centrifugal assembling setup with wireless force data acquisition system. Details of the setup are given in [5].

*Contacting Author: wen@acae.cuhk.edu.hk; phone: +852 2609 8475; fax: +852 2603 6002. This project is funded by a grant from the Hong Kong Research Grants Council (No. CUHK 4381/02).

composition) MUMPs fabricated mass-platform. The orientation of the chips were considered during the rotation-assembling process, i.e., the micro chips were placed perpendicular to the rotating axis, and the surface micromachined micro structures were faced outward as shown in Figure 1. With this configuration, the micro structures could be pulled away from the substrate once rotation was initiated. On-chip micro locking structures were used to prevent the micro structures from detaching from the substrate during rotation.

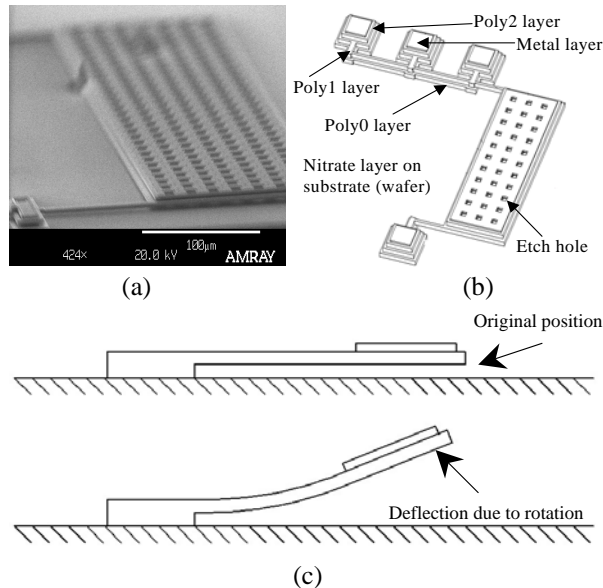


Figure 2. (a) SEM picture of a rotation sensor. (b) Illustration showing the multi-layered MUMPs structure used in our experiments. (c) Conceptual drawing for the side view of the rotation sensor.

III. SURFACE FORCE MEASUREMENT

To study the limitations of the centrifugal assembling method, systematic experiments were performed to ascertain the surface force interactions of the micro mass-platforms during the rotation assembling process. The structures tested consist of a simple mass platform supported by two cantilevers as shown in Figure 2. These platform-cantilever structures were designed as piezoresistive sensors capable of wirelessly transmitting motion information under rotation up to 6250rpm (similar to our prior work reported in [5]). Basically, these MUMPs rotation sensors can convert mechanical deflection of the polysilicon cantilevers into a change of electrical resistance, which can further be converted into a measurable change of voltage by connecting the sensors in a Wheatstone-bridge configuration. The voltage output from the bridge is then transmitted by a wireless transceiver after a voltage to frequency conversion. So, by using the setup as shown in Figure 1, the appropriate centrifugal force needed to *free* a structure that is initially adhered to the substrate by surface forces can be measured.

Representative dynamic motion of a structure as a function of the angular speed of a spinning disc is shown in Figure 3. The *freed-state* (defined as the state when a

platform is released from the substrate) is typically found at a high angular speed when the disc speed is increased. However, if the angular speed is decreased, the platform will *snap down* to the substrate at a lower angular speed than the *freed-state*. This hysteresis characteristic is repeatable and may be attributed to surface-force effects. The force required to free the structure is the force required to overcome the surface force for different size of masses.

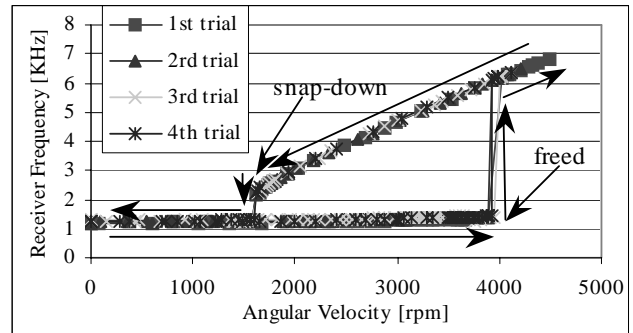


Figure 3. Typical motion of a platform suspended by two cantilever beams under rotation (receiver frequency is the wireless signal received and is proportional to the position of a platform).

The relationship between the *freed-state* and the *snap-down-state* of the platform is also analyzed for various platform geometries. In general, the *freed-state* angular speed is usually larger than *snap-down-state* angular speed as shown in Figure 4.

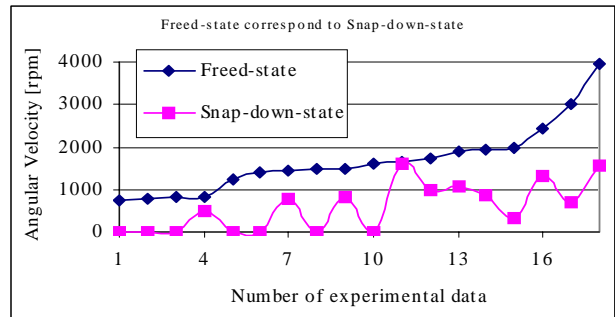


Figure 4. Comparison between *freed-state* and *snap-down-state*.

Although platform sizes as small as $320\mu\text{m} \times 160\mu\text{m}$ are all freed successfully, the range of required angular speed to free them is more sporadic than the large platforms (greater experimental error bars as shown in Figure 5). This phenomenon may be an indication of surface forces, which depend on many factors such as humidity and temperature, becoming more dominant as a mass becomes smaller.

IV. THEORETICAL FORCE ANALYSIS

Since experimental results indicated that interaction forces exist between the surface MEMS structures and the substrate, a theoretical comparison of the order of magnitude of forces between centrifugal force and the possible interaction forces, including van der Waals forces, capillary force and Casimir force, was carried out

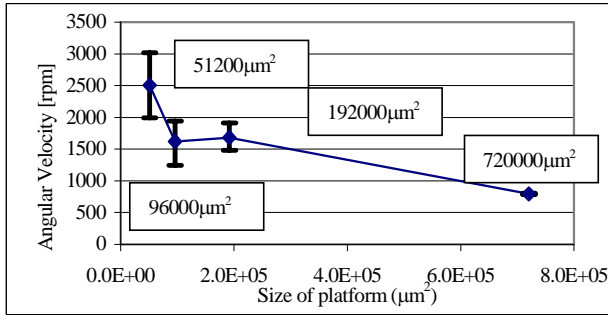


Figure 5. The freed-state for 4 different sizes of MUMPs platforms. The angular speed at which each platform type is freed from the substrate can be related to the centrifugal force acting on the micro platforms.

for the platform-cantilever structures. Since all the micro structures reported in this paper were fabricated by MUMPs, the run data on MUMPs43 and MUMPs46 were used to estimate the micro structure's parameters including the density and initial gap distance between micro structures and the substrate.

Van der Waals forces are well-known intermolecular forces between two atoms or small molecules as the distance (D) between them becomes very small. For the intermolecular forces model which was derived in [6], the overlap area between the mass-platform and substrate can be analogously modeled as two parallel surfaces and the equation of interaction energy (W) and pressure (P) is given in Eq. (2) and Eq. (3):

$$W_{two_surfaces} = \frac{A}{12 \cdot \pi \cdot D^2} \quad (2)$$

$$P_{two_surfaces} = \frac{A}{6 \cdot \pi \cdot D^3} \quad (3)$$

The resulting force should then be calculated by multiplying the pressure by the area (A) of the mass-platform, which is equal to the width of platform (W_{pf}) multiply by the length of platform (L_{pf}).

$$F_{two_surfaces} = P_{two_surfaces} \cdot W_{pf} \cdot L_{pf} \quad (4)$$

Casimir force [7] is another attractive force between two parallel neutral plates in vacuum when the plates are very close. It also depends on the plates' common area and distance:

$$F_{Casimir} = \frac{\pi^2}{240} \cdot \frac{h \cdot c}{D^4} \cdot A \quad (5)$$

where h is Planck constant, and c is speed of light.

Finally, capillary force can be a significant attractive force between 2 micro plates when the surrounding environment has enough humidity [8]. The capillary force depends on liquid-air interfacial tension (γ), contact angle (θ), radius of the liquid drop (r_1) and distance (D) between two surfaces, the following equation is the approximation made in [8],

$$F_{capillary}^{(1)} = \frac{2 \cdot \pi \cdot \gamma_1 \cdot \cos(\theta) \cdot r_1^2}{D} \quad (6)$$

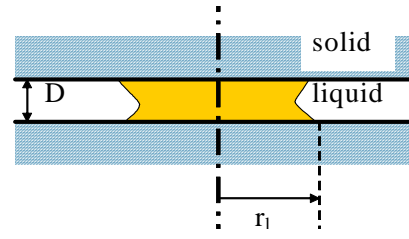


Figure 6. Illustration for two parallel surfaces for capillary force.

where γ_1 is between $0.1 - 10^{-3}$ N/m and approximated to be 7×10^{-3} N/m for surface MEMS structures.

However, (6) can be simplified into the following equation,

$$F_{Capillary}^{(2)} = \frac{4 \cdot \gamma \cdot A}{D} \quad (7)$$

where γ is the interfacial tension of water in air ($\sim 7.28 \times 10^{-4}$ N/m⁻¹ at room temperature).

However, since there are many etch holes on the mass-platforms for the MUMPs structures, so we modified (7) by multiplying a constant S_{factor} (which is less than 1) to account for the decrease in overall capillary force between a MUMPs platform and the substrate:

$$F_{Capillary}^{(3)} = \frac{4 \cdot \gamma \cdot A}{D} \cdot S_{factor} \quad (8)$$

To compare the relationship between centrifugal force and other interaction forces, the relationship between centrifugal force and the plate-to-substrate separation should be found first, i.e., equations (2) to (8) all depend on D . Hence, the deflection of beam supporting the mass-platform under applied centrifugal force should be ascertained. Using simple linear beam deflection theory, the deflection of the beam can be approximated as (refer to Figure 7):

$$Deflection = \frac{F_{centrifuga} \cdot L_{bm}^2}{12 \cdot E \cdot I_{bm}} \cdot (4 \cdot L_{bm} + 3 \cdot L_{pf}) \quad (9)$$

where E is Young's modulus (~ 169 GPa for polysilicon) and I_{bm} is the moment of inertia of the beam supporting the mass-platform. Note that, however, the total plate-to-substrate separation is the summation of the beam tip deflection and original gap ($Gap_{original}$) due to the sacrificial release fabrication process of MUMPs (approximately $2 \mu\text{m}$):

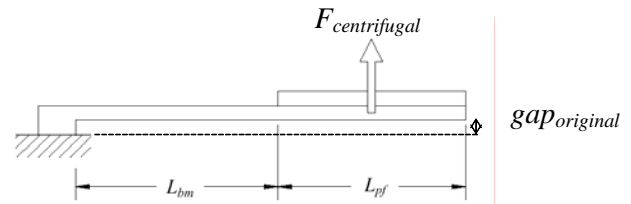


Figure 7. Schematic drawing of the side-view of the rotation sensor under upward equivalent concentrated force.

$$D = \text{Deflection} + \text{Gap}_{\text{original}} \quad (10)$$

By substituting the corresponding plate-to-substrate separation D in (10) to equations in (2) to (8), the order of magnitudes of the various surfaces can be compared. The capillary force is revealed as the dominating surface force as the gap distance between a plate structure and the substrate increases, i.e., van der Waals and Casimir forces are only significant when the gap distance is very small. In addition, as shown in Figure 8, when a MUMPs platform is rotated at a few thousand rpms, the centrifugal force acting on it is enough to overcome the capillary force between it and the substrate.

Since the capillary force is an attractive force between the mass-platform and the substrate, the centrifugal force must be large enough to overcome the capillary force, so that the micro structures can be raised and assembled. Assume the centrifugal force and capillary force (Eq. 8) are calculated independently without coupling between them, the intersection points of these forces for different sizes of mass platforms are shown in Figure 8.

Those intersection points were picked as the modeled results and compared with the experimental data as shown in Figure 9. It is observed that the general trend between the experimental and modeled results is similar. However, to provide a better fit between the two curves, more experiments data will need to be collected in a much better controlled environment, i.e., the humidity and temperature of the environment should be kept constant during the experiments. This is because the S_{factor} and γ are dependent on humidity and temperature.

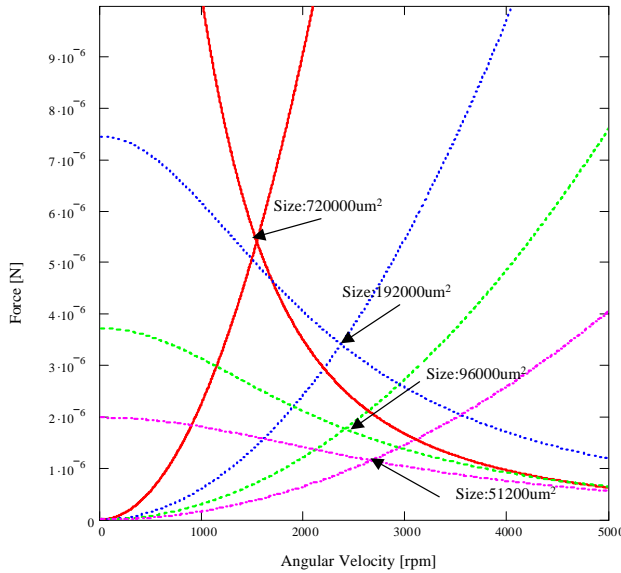


Figure 8. Comparison between centrifugal force and capillary force with different mass-platform size.

V. ASSEMBLY OF VERTICAL MICRO MIRRORS

A number of MUMPs structures that could potentially be used as micro mirrors were fabricated for centrifugal assembly experiments. These mirrors were classified into three types based on their platform sizes: 1) *Type I* mirrors

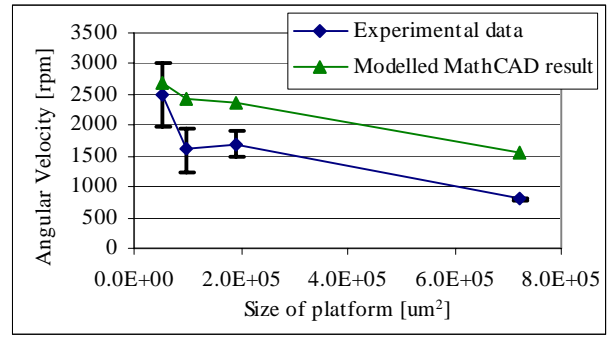


Figure 9. Freed-state comparison between experimental data and modeled result.

have dimensions of $600 \times 300 \mu\text{m}^2$, 2) *Type II* mirrors have dimensions of $300 \times 200 \mu\text{m}^2$, and 3) *Type III* mirrors have dimensions of $250 \times 100 \mu\text{m}^2$.

By increasing the angular speed, different sizes of mirrors were lifted up from horizontal to vertical position until they engaged with designed latches were engaged. When the rotation system reached the maximum angular speed of about 6250rpm (a limitation of our current rotation system), most of the *Type I* micro mirrors have locked successfully into vertical position. Since centrifugal force applied on larger masses is greater than smaller masses at a given angular speed, *Type I* mirrors could be assembled at a smaller angular speed than *Type II* and *Type III* mirrors. When angular speed is at 6250rpm, the centrifugal forces applied on *Type I*, *Type II* and *Type III* mirrors are approximately to be $2.23 \times 10^{-5} \text{N}$, $7.45 \times 10^{-6} \text{N}$ and $3.10 \times 10^{-6} \text{N}$, respectively. In Figure 10, arrays of assembled micro mirrors are shown after a MUMPs chip was rotated using our centrifugal assembly system.

By counting the number of assembled micro mirrors for all three types of mirrors with respect to increment of angular speed at 1200rpm, the yield of the centrifugal processes was studied (as shown in Figure 11). The percentage of each type of lifted micro mirror as a function of angular speed is shown in Figure 12. *Type I* micro mirrors started to be lifted (*freed-state*) at about 1200rpm. On the other hand, *Type II* and *Type III* started to be lifted at greater angular speeds.

Since *Type III* micro mirrors have the smallest mass, a minimum of 4800rpm was needed to assemble the first mirror. The fact that even the same size of mirrors were assembled at different angular velocities can be explained by the presence of other counter-acting forces such as frictional force between the hinges and the rotating platforms and also the capillary force between the mass platforms and the substrate. All *Type I* mirrors were lifted under 4800rpm. About 50% of *Type II* mirrors were lifted at this angular speed, and more than 90% were lifted when the angular speed reached 6250rpm. The percentage of *Type III* platforms lifted increased from zero to 22% at 6250rpm.

In summary, the success rate in lifting up all the micro mirrors was about 70% when angular speed reached 6250rpm as shown in Figure 13. The success rate can potentially be increased by increasing angular speed or rotational radius of the disc because larger centrifugal force can then be applied on *Type III* micro mirrors.

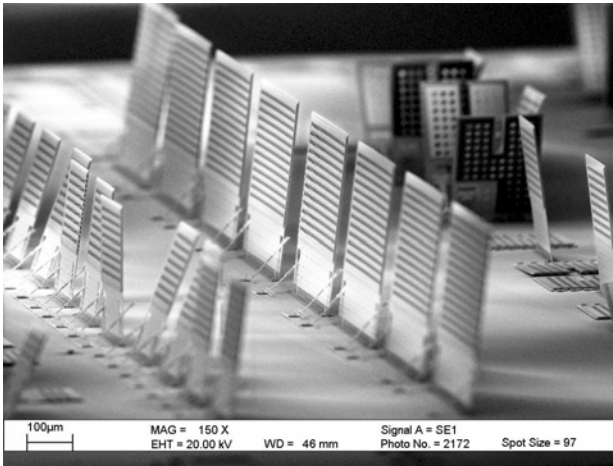


Figure 10. SEM picture of the batch micro-assembled micro mirror arrays.

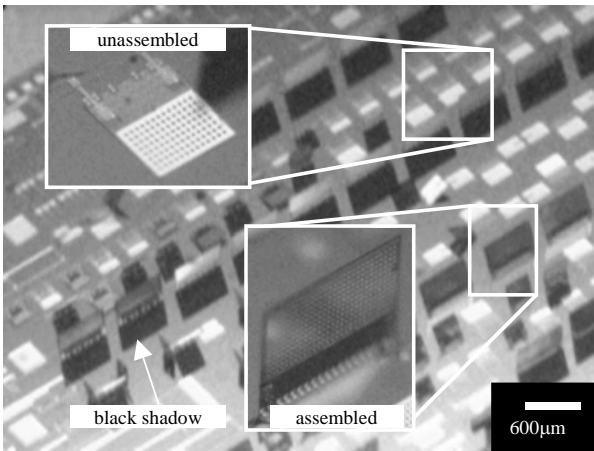


Figure 11. Different sizes of micro mirrors assembled by centrifugal force. The white structures in the picture represent the unassembled structures (the white color is due to reflection from gold layer as observed under a 3D microscope), and the gray structures are the assembled structures with black shadows.

The centrifugal self-assembly process was verified to be very successful and gave high yield. None of the micro mirrors were damaged (see Figure 10 for example) during the assembling process because the applied centrifugal force was small ($\sim 2 \times 10^{-5} \text{ N}$ for Type I platforms, based on Eq. 1) and did not exceed the maximum tensile strength of polysilicon hinges holding the platforms (refer to our prior work reported in [9]).

VI. ASSEMBLY OF MOVABLE MICRO MIRRORS

Movable (2-Dimensional) micro mirrors were also designed and built using MUMPs process to illustrate that the centrifugal assembly technique can be applied to assemble complex structures. One unassembled 2D micro mirror of such design is shown in Figure 14. The center part of the structure shown in the figure is the mirror plane which is $200 \times 200 \mu\text{m}^2$ and can be used to perform light-wave reflection. It is surrounding by the supporting structural frame and 8 identical lockers, the overall size is

about $1000 \times 1000 \mu\text{m}^2$ (not including the electrical bond pads). The mirror plane is needed to be lifted up so that sufficient space between the mirror and substrate could be provided for the mirror to move up and down

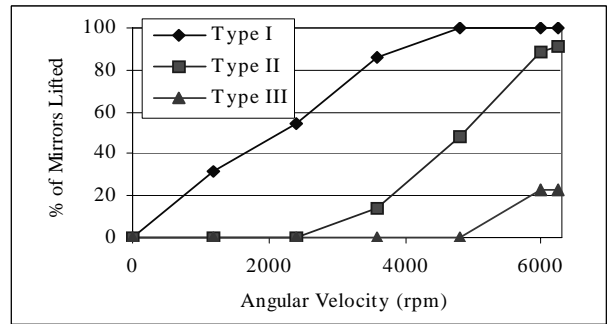


Figure 12. Percentage of micro platforms lifted versus angular speed, with platform size as a parameter.

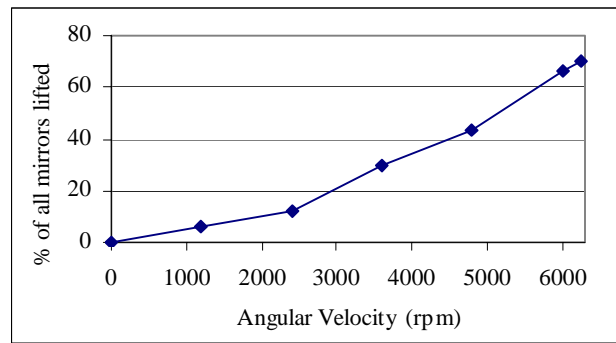


Figure 13. Percentage of mirrors lifted on a MUMPs43 chip.

(perpendicular to substrate plane). When the mirror moves, impinging light-wave can be reflected to different directions, hence the mirror can be used as an optical ON/OFF or channel switch. This 2D micro mirror can be driven by applying an electrostatic force (voltage) between the mirror plane and the substrate.

To test these structures, 3×6 micro mirrors were fabricated on each die ($1 \text{ cm} \times 0.5 \text{ cm}$). One row of micro mirrors was used as “control micro mirrors” that could not be lifted (i.e., they were not sacrificially released) during assembly as shown in Figure 15.

Six identical dies were tested by the centrifugal assembly system running between 4300rpm–4700rpm angular speed. Note that the radius of the rotational disc used for this batch of assembly is larger than the disc used in assembling the vertical micro mirrors, hence the angular speed needed to lift these movable 2D micro mirrors can not be compared with the speeds given in the previous section. Not including the control micro mirrors, a totally of 90 micro mirrors were tested. The results are summarized in Table 2.

Although the yield of the fully assembled 2D micro mirrors (as shown in Table 1) is not as high as the vertical micro mirrors, it is still a very good result compare to other existing techniques used to assemble these type of structures, e.g., using on-chip actuators to assemble these structures have also about 25% success rate. In addition, using micro manipulation probes to lift up these structures manually is very difficult because unbalanced or

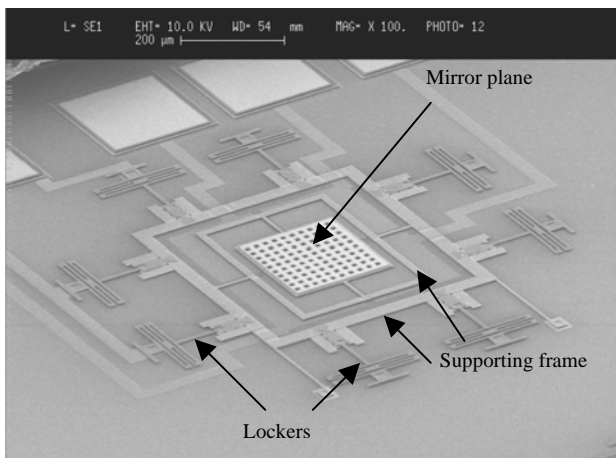


Figure 14. Isometric view of unassembled 2D micro mirror.

excessively large force will damage these structures easily. Besides, at least 30% of these structures were partly assembled, i.e., at least one of the latches did not lock, which implies that if the angular speed of the rotation disc can be increased to produce a larger centrifugal force, then the yield could potentially be increased to greater than 60%. After centrifugal assembly, these micro mirrors were measured to be 75-85 μ m above the substrate. An SEM picture of an assembled mirror is shown in Figure 16. The micro mirrors were successfully tested to move up and down by the applying AC voltages between 50-80V.

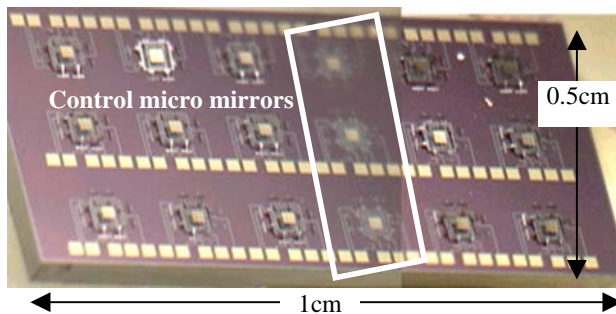


Figure 15. 2D micro mirror arrays on each die. One row (shown in the white box) is used as reference micro mirrors.

VII. CONCLUSION

Non-contact batch micro-assembly of MUMPs micro structures using centrifugal force was demonstrated. Various MUMPs micro mirrors were rotated about micro hinges centrifugal force and vertically locked by latches. Results showed that batch micro assembly by centrifugal force is low-cost and reliable, and give 100% yield when assembling micro mirrors with 600 μ m \times 300 μ m \times 4 μ m dimensions without destroying any micro structures. Another kind of dynamic 2D micro mirror structure was also successfully assembled using the same process. These mirrors structures were also actuated successfully after centrifugal assembling. The assembling process reported in this paper is very low-cost and non-destructive, thus it will provide MOEMS engineers with a quick and convenient way to assemble 3D MOEMS components and devices.

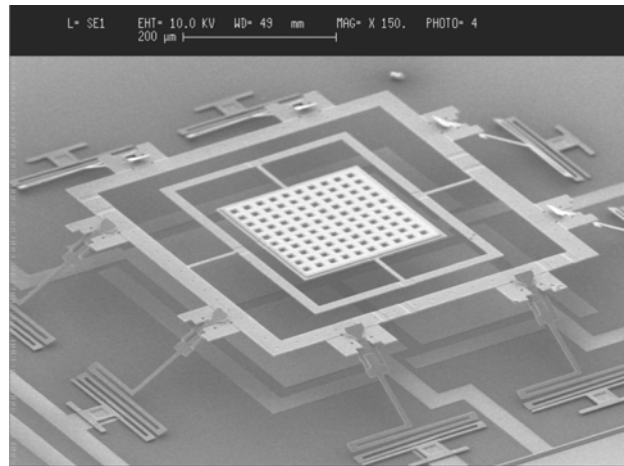


Figure 16. Fully assembled 2D micro mirror.

Table 1. Results of centrifugal assembly on 2D micro mirrors.

Result	No.	Percentage
8 locked (fully assembled)	23	25.56%
4-7 locked (partly assembled)	32	35.56%
1-3 locked (partly assembled)	2	2.22%
Not lifted	18	20.00%
Broken	15	16.67%
Total tested micro mirrors	90	100%

ACKNOWLEDGMENT

We would like to thank Prof. Zhao Pu-Ya (State Key Laboratory of Nonlinear Mechanics, Institute of Mechanics, Chinese Academy of Sciences) who provided the approximate equations of capillary force between a surface MEMS structure and the substrate.

REFERENCES

- [1] E. E. Hui, R. T. Howe, and M. S. Rodgers, "Single-Step Assembly of Complex 3-D Microstructures", *Proc. of the 13th IEEE Int. Conf. on MEMS*, pp. 602-607, 2000.
- [2] T. Akiyama, D. Collard, and H. Fujita, "Scratch drive actuator with mechanical links for self-assembly of three-dimensional MEMS", *J. Microelectromechanical Systems*, vol. 6, Issue. 1, pp. 10-17, 1997.
- [3] R. R. A. Syms, "Equilibrium of hinged and hingeless structures rotated using surface tension forces", *J. Microelectromechanical Systems*, vol. 4, Issue. 4, Dec., pp. 177-184, 1995.
- [4] V. Kaajakari and A. Lal, "Electrostatic Batch Assembly of Surface MEMS Using Ultrasonic Triboelectricity", *Proc. of the 14th IEEE Int. Conf. on MEMS*, pp. 10-13, 2001.
- [5] W. J. Li, T. Mei, and W. Sun, "A Micro Polysilicon High-Angular-Rate Sensor with Off-Chip Wireless Transmission", *Sensors and Actuators A: Physical*, 89, 1-2, pp. 56-63, 2001.
- [6] Jacob Israelachvili, *Intermolecular & Surface Forces*, 2nd Edition, 1991.
- [7] Y. P. Zhao and W. J. Li, "Surface Stability of Expitaxial Elastic Films by Casimir Force", *Chinese Physics Letter*, vol. 19, No. 8, August 2002, pp. 1162-1163.
- [8] C. H. Mastrangelo, C. H. Hsu, "Mechanical Stability and Adhesion of Microstructures Under Capillary Forces", *J. Microelectromechanical Systems*, vol. 2, No. 1, March 1993.
- [9] K. W. C. Lai, A. P. Hui, and W. J. Li, "Non-Contact Batch Micro-Assembly by Centrifugal Force", *Proc. of the 15th IEEE Int. Conf. on MEMS*, pp. 184-187, 2002.